

Cite this: *J. Mater. Chem. A*, 2022, 10, 19914

## Design and development of nucleobase modified sulfonated poly(ether ether ketone) membranes for high-performance direct methanol fuel cells†

Juan Wu,<sup>ab</sup> Shijun Nie,<sup>ab</sup> Hai Liu,<sup>b</sup> Chunli Gong,<sup>\*b</sup> Quanyuan Zhang,<sup>ID \*a</sup> Zushun Xu<sup>ID a</sup> and Guangfu Liao<sup>ID \*c</sup>

The development of low-cost and high-performance proton exchange membranes (PEMs) for direct methanol fuel cell (DMFC) applications is a promising solution to the energy shortage. In this work, a series of sulfonated poly(ether ether ketone)s (SPEEKs) modified with two nucleobases, adenine (A) and cytosine (C) with different degrees of substitution, SPEEK-A<sub>x</sub> and SPEEK-C<sub>x</sub> were successfully synthesized. The basic sites of A and C can immobilize phosphoric acid (PA) molecules through acid–base interaction to fabricate PA-doped SPEEK membranes. In addition, the formation of ionic crosslinking caused by basic sites enhances the thermal stability and mechanical strength of the PA-doped membranes. As a result, the SPEEK-A<sub>x</sub>/PA and SPEEK-C<sub>x</sub>/PA membranes possess satisfactory strength (>23.5 MPa) even if their elongation at break remained at a very high level (>200%) in the hydrated state. These PA-doped membranes exhibited ultra-high proton conductivities (all beyond 220 mS cm<sup>-1</sup>) at 80 °C, while the conductivity of SPEEK was only 43.8 mS cm<sup>-1</sup> with similar IEC values. This may be attributed to the acid–base pairs between the acidic sites (–SO<sub>3</sub>H and H<sub>2</sub>PO<sub>4</sub><sup>-</sup>) and basic sites, which can serve as efficient transportation paths for proton migration. Furthermore, the ionic crosslinked structure decreased the methanol crossover of the membranes. The SPEEK-C<sub>50</sub>/PA membrane possesses outstanding DMFC performance with a maximum power density of 141.7 mW cm<sup>-2</sup> when fed with 2 M methanol at 80 °C, more than twice as much as that of SPEEK (67.2 mW cm<sup>-2</sup>) and Nafion 115 (64.1 mW cm<sup>-2</sup>), which outperforms the majority of previously reported Nafion and SPEEK membranes. Therefore, the prepared nucleobase modified PEMs showed promising potential for high-performance DMFC application.

Received 20th April 2022  
Accepted 23rd May 2022

DOI: 10.1039/d2ta03166c

rsc.li/materials-a

<sup>a</sup>Ministry of Education Key Laboratory for the Green Preparation and Application of Functional Materials, Hubei Key Laboratory of Polymer Materials, School of Materials Science and Engineering, Hubei University, Wuhan 430062, China. E-mail: qyzhang142918@hotmail.com

<sup>b</sup>School of Chemistry and Materials Science, Hubei Engineering University, Xiaogan, Hubei, 432000, China. E-mail: chunli.gong@hbeu.edu.cn

<sup>c</sup>Engineering Research Center of Nano-Geomaterials of Ministry of Education, China University of Geosciences, Wuhan 430074, China. E-mail: liaogf@mail2.sysu.edu.cn

† Electronic supplementary information (ESI) available. See <https://doi.org/10.1039/d2ta03166c>



Prof. Guangfu Liao received his PhD degree in Material Physics & Chemistry from Yat-sen University in 2020. Then he joined the laboratory of Prof. Yi-Chun Lu at The Chinese University of Hong Kong and worked as a Research Associate. Now, he is a Researcher at the China University of Geosciences. His research interests involve Polymer Synthesis & Applications, Polymer Membranes, Redox Flow Batteries, Nanoporous & Nanostructured Materials, Photo- & Electro-Catalysis, Biomaterials, Gas Storage & Energy Conversion, etc. So far, he has published more than 50 high profile SCI papers including *Matter*, *Progress in Materials Science*, *Energy & Environmental Science*, *Trends in Chemistry*, *Chemical Science*, *ACS Catalysis*, *Nano Energy*, *Small*, *Journal of Materials Chemistry A*, *Macromolecules*, etc.

# 1. Introduction

Direct methanol fuel cells (DMFCs) have great application prospects in portable electronic equipment, mobile power and electric vehicles, due to their high energy power density, rich sources of liquid methanol, convenient fuel storage and transportation, low environmental pollution and quick start-up.<sup>1–5</sup> As a key component of DMFCs, a proton exchange membrane (PEM) is mainly used to block anode and cathode reactants and conducting protons, which has significant impact on the performance of the fuel cell. Currently, the most commercially utilized PEM is a perfluorosulfonic acid membrane, such as Nafion developed by DuPont in the 1960s, which has high proton conductivity and good chemical, mechanical, and thermal stability.<sup>6,7</sup> However, the Nafion membrane also has high methanol permeability ( $\sim 10^{-6}$  cm<sup>2</sup> s<sup>-1</sup>) and drastically decreases the performance of the fuel cell.<sup>8</sup> In addition, the high cost of Nafion also impedes the commercial application of DMFCs.<sup>9,10</sup> Therefore, the development of low-cost and high-performance PEMs alternative to Nafion membranes has attracted extensive attention in the past few decades.

Sulfonated poly(ether ether ketone)s (SPEEKs) have been explored as a promising alternative to commercial Nafion for DMFC applications due to their relatively low cost, high proton conductivity, sufficient mechanical strength and appropriate thermal stability, as well as low methanol permeability.<sup>11–13</sup> However, the proton conductivity, methanol resistance, and mechanical properties of SPEEK membranes are closely related to the degree of sulfonation (DS). SPEEK membranes with low DS have low proton conductivity. With the increase of DS, the proton conductivity increases, which will also increase the swelling of the membranes, reduce their mechanical properties and dimensional stability, and dramatically decrease the lifetime of the fuel cell.<sup>14–16</sup> In order to overcome these disadvantages, two kinds of polymer modification methods have been used to modify SPEEK membranes by researchers including polymer blending<sup>17–19</sup> and crosslinking.<sup>20–23</sup> SPEEK membranes crosslinked to a certain extent *via* chemical or ionic crosslinking can not only overcome the membrane swelling problem caused by high DS, but also inhibit methanol crossover due to the dense network structure formed by crosslinking.<sup>24</sup>

Acid–base compositing, a convenient approach of ionic crosslinking, has been reported to improve the performance of PEMs through acid–base interactions between the acidic groups (*e.g.*, SO<sub>3</sub>H groups) and basic groups (*e.g.*, N-atom-containing groups) in the polymer chain.<sup>25,26</sup> Thus, blending of a basic polymer containing N-heterocycles with a sulfonic acid polymer is conducive to reducing membrane swelling, improving mechanical properties and decreasing the methanol crossover of membranes.<sup>27–31</sup> Various researches have been reported on composite membranes of SPEEK with imidazole-group-containing polymers, particularly poly(benzimidazole) (PBI), which showed low methanol crossover.<sup>32–34</sup> For example, Li *et al.* reported that, by increasing the content of PBI from 2.5 to 15%, the methanol crossover of the membranes decreased from  $7.92 \times 10^{-7}$  to  $3.10 \times 10^{-7}$  cm<sup>2</sup> s<sup>-1</sup>. Unfortunately, the proton conductivity also reduced from  $1.8 \times 10^{-1}$  to  $1.0 \times 10^{-1}$  S cm<sup>-1</sup>.<sup>34</sup> In

addition, some drawbacks such as decreased water uptake and inhomogeneity of the blend caused by the poor processability of PBI have limited the use of PBI blended membranes.<sup>35</sup>

Nucleobases such as adenine (A) and cytosine (C), the main components of base pairs in deoxyribonucleic acid (DNA), are composed of nitrogenous heteroatomic rings with ionic sites and have good thermal stability up to 250 °C, and can be expected to act as proton charge carriers in PEMs under anhydrous conditions. However, it is difficult to directly utilize DNA as PEMs due to their high water solubility and poor mechanical properties.<sup>36</sup> The introduction of a nucleobase unit into the polymer backbone is an interesting strategy and only a few reports have appeared so far.<sup>37,38</sup> In this work, two nucleobase units, A and C, were incorporated into the SPEEK backbone, and the structures of the resulting nucleobase modified SPEEKs (SPEEK-A<sub>x</sub> or SPEEK-C<sub>x</sub>) were characterized by <sup>1</sup>H NMR and FTIR. A and C functionalized SPEEKs can form ionic cross-linking between basic N atoms and SO<sub>3</sub>H groups through acid–base interaction, which inhibit the swelling of the membrane and improve the mechanical properties. In addition, after doping with phosphoric acid (PA), abundant acid–base pairs are developed between acidic phosphate ions and basic aromatic nitrogen heterocycles together with NH groups in membranes, which can serve as efficient proton transfer active sites to enhance proton conductivity.<sup>39</sup> The physicochemical properties of the phosphoric acid doped membranes, including swelling behavior, thermal and mechanical properties, methanol permeability and proton conductivity, were investigated in detail. Additionally, the DMFC performance based on the obtained membranes has been explored and compared with that of commercial Nafion 115, modified Nafion and other previous SPEEK membranes.

## 2. Experimental section

### 2.1 Materials

Poly(ether ether ketone) (PEEK 021P) was purchased from Jilin Jusep Special Plastics Co., Ltd (China). Adenine (A, 98%) and dimethyl sulfoxide (DMSO) were purchased from Macklin. Cytosine (C, 98%) and *N,N'*-carbonyldiimidazole (CDI, 98%) were purchased from Aladdin Reagent Co., Ltd (China). Methanol was purchased from Fluton Biochemical Technology Co., Ltd (China). Concentrated sulfuric acid (conc. H<sub>2</sub>SO<sub>4</sub>, 98%), *N,N*-dimethylformamide (DMF) and phosphoric acid (H<sub>3</sub>PO<sub>4</sub>, 85%) were purchased from Sinopharm Chemical Reagent Co., Ltd (China). All chemical reagents were analytical grade and used without further purification.

### 2.2 Synthesis of SPEEK

SPEEK was synthesized *via* direct electrophilic sulfonation of PEEK by using conc. H<sub>2</sub>SO<sub>4</sub> according to the literature.<sup>40</sup> In a three-neck flask, 10 g of PEEK was dissolved in 190 mL of conc. H<sub>2</sub>SO<sub>4</sub> at 50 °C and an orange solution was obtained. After reacting for 5 h, the resultant solution was cooled to room temperature, followed by pouring into ice water slowly with stirring using a glass rod. White filamentous precipitations were collected and washed with deionized water to neutral. The

polymer was dried in an air blowing oven at 60 °C for 48 h and SPEEK with a sulfonation degree of 60% (determined by  $^1\text{H}$  NMR) was obtained.

### 2.3 Synthesis of nucleobase modified SPEEKs

Nucleobase modified SPEEKs were synthesized from SPEEK and different nucleobases (A or C) according to the literature.<sup>21</sup> SPEEK-A<sub>30</sub> is given as an example. To a 100 mL three-necked flask, equipped with a magnetic stirrer, 3.0 g of dried SPEEK (5.35 mmol of  $\text{SO}_3\text{H}$ ) and 30 mL of DMSO were charged. After the polymer was completely dissolved at 60 °C, 0.2864 g of CDI (1.76 mmol) was added and stirred for 3 h, and then 0.2170 g of adenine (1.60 mmol) was added and reacted for another 3 h. The resultant solution was precipitated in deionized water and the precipitation was collected by filtration, washed thoroughly with water, and dried in an oven at 60 °C for 48 h. A series of nucleobase modified SPEEKs with different nucleobase contents (SPEEK-A<sub>10</sub>, SPEEK-A<sub>50</sub>, SPEEK-C<sub>10</sub>, SPEEK-C<sub>30</sub> and SPEEK-C<sub>50</sub>) were also synthesized by adjusting the amount of CDI and nucleobase (A or C).

### 2.4 Fabrication of membranes and their phosphoric acid (PA) doping

The fabrication of PA-doped SPEEK-A<sub>x</sub> and SPEEK-C<sub>x</sub> membranes is illustrated in Scheme 1. Nucleobase modified

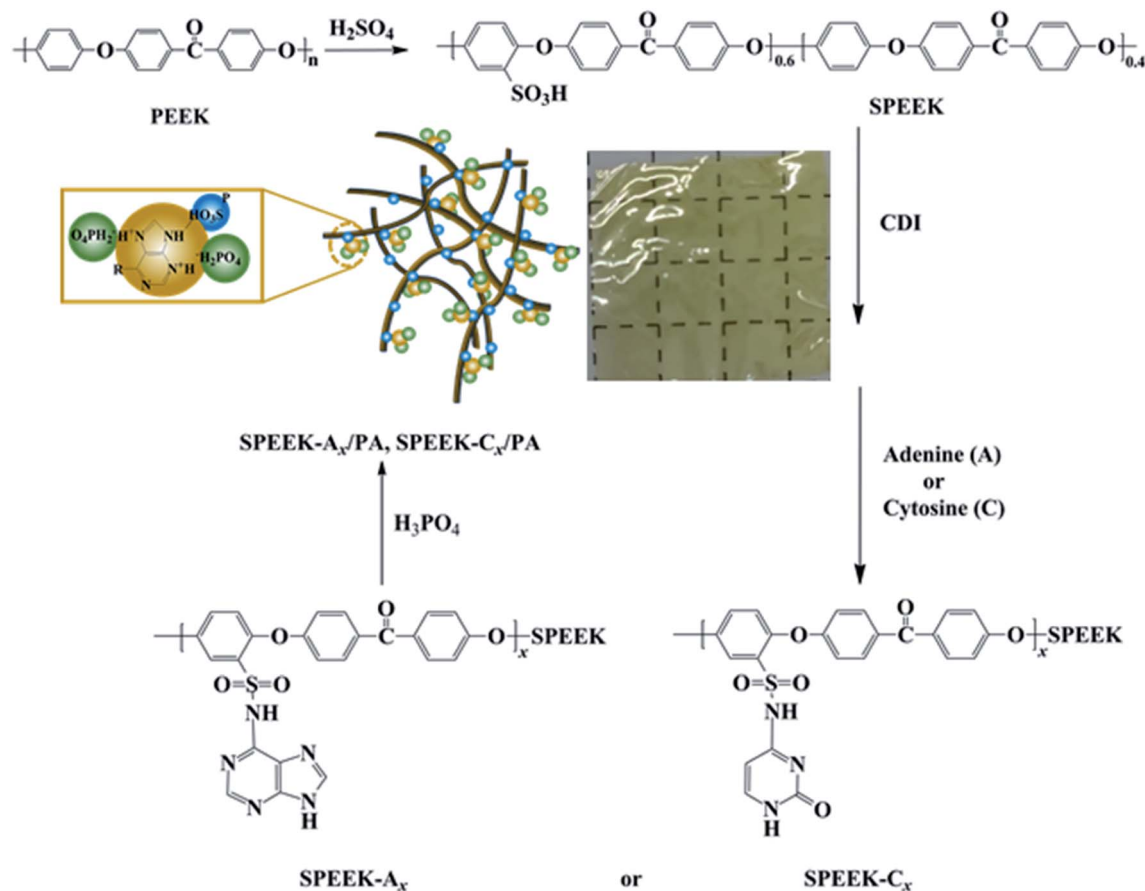
SPEEKs were dissolved in DMF to form an 8 wt% solution. The solution was cast onto a clean glass plate, followed by drying for 12 h at 40 °C in an oven to produce the membranes, which were further dried at 80 °C for another 12 h to remove excess solvent. The thicknesses of the obtained membranes were about 60 ± 5 μm.

Dried polymer membranes were immersed in 85 wt% PA at 60 °C for 72 h until the weight of the membrane remains unchanged, and PA doping polymer membranes were obtained by wiping the excess PA adsorbed on the surface with filter papers. The PA doping uptake and acid doping level (ADL) of the membranes were performed at least three times with different pieces to examine the reproducibility. The ADL is the number of phosphate molecules adsorbed by each repeating unit of the polymer, and the ADL was calculated by the following equation:

$$\text{ADL} = \frac{(W_w - W_d)/M_{\text{PA}}}{W_d/M_{\text{P}}}$$

where  $W_d$  and  $W_w$  represent the masses before and after PA doping of the membranes, and  $M_{\text{PA}}$  and  $M_{\text{P}}$  are the molecular weights of PA and the repeating unit of the polymer, respectively. The measurements of three duplicates were carried out for consistency checking.

The sample characterization and performance tests including water uptake, swelling ratio, ion exchange capacity,



Scheme 1 Preparation of PA doping SPEEK-A<sub>x</sub> and SPEEK-C<sub>x</sub> membranes.

proton conductivity, methanol permeability, and acidic direct methanol fuel cell performance are shown in detail in the ESI.†

### 3. Results and discussion

#### 3.1 Characterization of pristine and nucleobase modified SPEEKs

SPEEK was synthesized by a post-sulfonation procedure of PEEK with concentrated  $\text{H}_2\text{SO}_4$ . Fig. 1a shows the  $^1\text{H}$  NMR spectrum of SPEEK, and the peak at 7.50 ppm is assigned to the *ortho*-CH- ( $\text{H}_e$ ) of the sulfonate substituted benzene ring. According to the ratio between the integrated peak area of the  $\text{H}_e$  signal and the peak area of the signals at 7.70–7.85 ppm ( $\text{H}_{a+a'}$ ), the calculated DS was about 60%. CDI was used to partially activate the  $\text{SO}_3\text{H}$  group of SPEEK, followed by reacting with nucleobase (A and C) to obtain nucleobase modified SPEEKs (SPEEK-A<sub>x</sub> and SPEEK-C<sub>x</sub>). The chemical structures were also confirmed by  $^1\text{H}$

NMR spectra, as shown in Fig. 1a. The chemical shifts of the hydrogen attributed to  $-\text{SO}_2\text{NH}-$  ( $\text{H}_i$ ) appear near 9.08 ppm for both adenine and cytosine functionalized SPEEKs. And the characteristic peaks of the hydrogen assigned to  $-\text{NH}-$  ( $\text{H}_j$ ) of the aromatic heterocycle for adenine and cytosine are observed at 8.46 and 8.25 ppm, respectively. The peaks at 7.72 and 8.44 ppm are assigned to the  $-\text{CH}-$  ( $\text{H}_f$  and  $\text{H}_g$ ) of the five and six membered rings for adenine unit, respectively. And the peaks observed at 5.93 and 5.91 ppm are ascribed to the  $-\text{CH}=\text{CH}-$  ( $\text{H}_g$  and  $\text{H}_g'$ ) of the pyrimidine ring for cytosine. All these characteristic peaks indicate that both adenine and cytosine are successfully incorporated into the SPEEK backbone.

FTIR spectra were also used to confirm the chemical structures of the pristine and modified SPEEKs, as shown in Fig. 1b. The asymmetric and symmetric stretching vibrations assigned to the  $\text{SO}_3\text{H}$  group are observed at  $1094\text{ cm}^{-1}$  and  $1019\text{ cm}^{-1}$ . The peaks that appeared near  $1650\text{ cm}^{-1}$  and  $1220\text{ cm}^{-1}$  correspond to the  $\text{C}=\text{O}$  group and  $\text{C}-\text{O}$  bonds for the SPEEK backbone, respectively. And the peaks at  $1591\text{ cm}^{-1}$  and  $1495\text{ cm}^{-1}$  are ascribed to the characteristic skeleton vibrations of aromatic rings.<sup>41</sup> After adenine and cytosine are introduced into SPEEK, two new characteristic peaks emerge near  $1475\text{ cm}^{-1}$  and  $1075\text{ cm}^{-1}$ , which can be attributed to the stretching vibrations of sulfonamide groups. And the out-of-plane bending vibrations of  $\text{C}-\text{H}$  groups for purine and pyrimidine rings (about  $845\text{ cm}^{-1}$ ) are overlapped by the  $\text{C}-\text{H}$  bending vibration of the aromatic ring at  $840\text{ cm}^{-1}$ . Interestingly, the asymmetric stretching vibration peaks of  $\text{SO}_3\text{H}$  groups ( $1094\text{ cm}^{-1}$ ) almost disappear, indicative for ionic crosslinking between  $\text{SO}_3\text{H}$  groups and basic adenine or cytosine units through acid–base interaction.<sup>42</sup> When PA is doped, the intensities of the  $\text{SO}_3\text{H}$  stretching vibration at  $1019\text{ cm}^{-1}$  and  $\text{SO}_2\text{NH}$  characteristic vibration at  $1075\text{ cm}^{-1}$  decrease and a weak signal can be observed at  $1105\text{ cm}^{-1}$ , and it infers the formation of acid–base pairs between PA molecules and the basic  $\text{NH}$  groups from sulfonamide groups, purine and pyrimidine rings.<sup>43</sup>

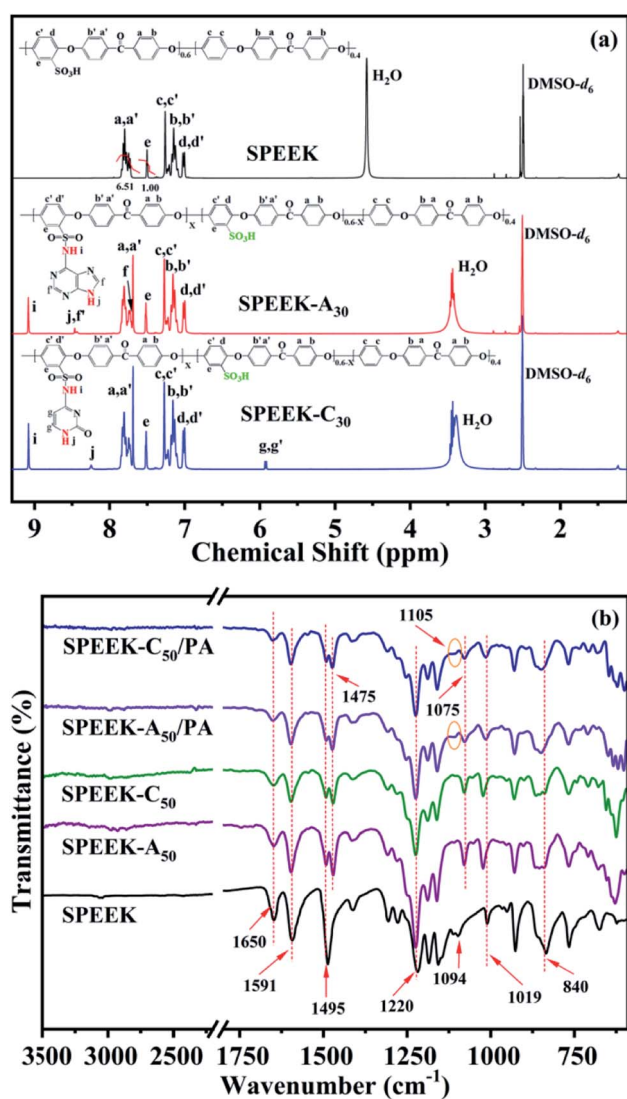


Fig. 1 (a)  $^1\text{H}$  NMR spectra of SPEEK, SPEEK-A<sub>30</sub> and SPEEK-C<sub>30</sub> in  $\text{DMSO}-d_6$ . (b) FTIR spectra of SPEEK, SPEEK-A<sub>50</sub> (or C<sub>50</sub>) and SPEEK-A<sub>50</sub> (or C<sub>50</sub>)/PA.

#### 3.2 Phosphoric acid (PA) doping level

As previously reported,<sup>44</sup> the PA doping level has a strong influence on proton transport in PEMs. Generally, for mere PA-doped alkaline polymers (represented by PBI), high PA uptake means more PA molecules including bonded PA through basic groups as well as free PA can participate in the process of proton migration. However, high PA loading inevitably results in severe leaching of PA especially in a humidified environment. Therefore, PA-doped PEMs are usually used in high-temperature PEMFCs, but rarely as low-temperature polymer electrolytes. In this work, two kinds of biological bases were introduced into SPEEK backbones to provide PA adsorption sites and the PA doping level was tested using the PA uptake and acid doping level (ADL) (as shown in Table 1). For the SPEEK-A<sub>x</sub>/PA membranes, the PA uptake and ADL slightly increased up to 64.7% and 2.4 with the grafting content of adenine, mainly due to the introduced more basic sites. As for the SPEEK-C<sub>x</sub>/PA membranes, they did not exhibit an obvious increase in the PA uptake values. Such a phenomenon may be related to the



Table 1 PA uptake, ADL, hydration coefficient ( $\lambda$ ), and mechanical properties of SPEEK, SPEEK- $A_x$ /PA and SPEEK- $C_x$ /PA membranes

| Samples             | PA uptake (%) | ADL | $\lambda$ | Tensile strength (MPa) |            | Elongation at break (%) |       |
|---------------------|---------------|-----|-----------|------------------------|------------|-------------------------|-------|
|                     |               |     |           | Dry                    | Wet        | Dry                     | Wet   |
| Nafion 115          | —             | —   | —         | 30.4 ± 2.2             | 25.8 ± 0.3 | 294.4                   | 315.2 |
| SPEEK               | —             | —   | 7.8       | 68.7 ± 4.9             | 25.3 ± 0.7 | 92.0                    | 120.2 |
| SPEEK- $A_{10}$ /PA | 55.8          | 2.1 | 15.5      | 76.8 ± 4.5             | 23.7 ± 3.2 | 251.1                   | 251.0 |
| SPEEK- $A_{30}$ /PA | 56.0          | 2.1 | 15.0      | 74.0 ± 3.4             | 28.1 ± 2.7 | 207.5                   | 218.4 |
| SPEEK- $A_{50}$ /PA | 64.7          | 2.4 | 14.2      | 70.3 ± 0.2             | 30.7 ± 2.1 | 237.9                   | 301.5 |
| SPEEK- $C_{10}$ /PA | 51.2          | 2.0 | 13.2      | 78.1 ± 7.1             | 36.5 ± 2.8 | 210.1                   | 195.9 |
| SPEEK- $C_{30}$ /PA | 56.3          | 2.1 | 14.9      | 76.4 ± 4.8             | 35.4 ± 8.7 | 199.3                   | 307.8 |
| SPEEK- $C_{50}$ /PA | 56.0          | 2.1 | 18.1      | 76.6 ± 4.7             | 36.6 ± 6.6 | 153.0                   | 323.8 |

electron receptor effect of carbonyl ( $-C=O$ ), which decrease the basicity of the  $-NH$  group in the unit of cytosine. Overall, the PA uptake and ADL of these two kinds of zwitterionic polymers both remained at a low level.

### 3.3 Thermal properties

Thermal stability is important for the durability of a PEM because it should withstand hot pressing to prepare the membrane electrode assembly (MEA) and long-term operation at different temperatures. Fig. 2 shows the TGA curves of SPEEK, SPEEK- $A_x$ /PA, and SPEEK- $C_x$ /PA to compare their thermal stability in the temperature range of 100–800 °C at a heating rate of 10 °C min<sup>-1</sup> in a N<sub>2</sub> atmosphere. No weight loss around 100 °C can be found because the isothermal pretreatment of the membranes at 100 °C removed the physically absorbed water. Pristine SPEEK showed a three-step weight loss behavior: the first stage in the range of 195–270 °C is considered to be the volatilization of the hydrogen-bonded water and a small amount of residual DMF solvent. The second step from 285 to 400 °C is the decomposition of sulfonic acid groups, and the last step is the degradation of the main chains of SPEEK. In the case of PA-doped membranes, two weight loss steps were observed. The first weight loss, including the dehydration of PA and hydrogen-bonded water, started later at about 250 °C and

overlapped with the stage of the  $-SO_3H$  groups splitting-off. Moreover, the degradation of SPEEK- $A_x$  and SPEEK- $C_x$  main chains obviously moved to higher temperature when compared to that of SPEEK, mainly due to the formed sulfonamide ionic bond and other ionic interactions between acid groups and basic sites. The TGA result proved that these PA-doped membranes are thermally stable enough to be used as PEMs in PEMFCs and DMFCs.

### 3.4 Mechanical properties

Sufficient mechanical strength of PEMs is essential for the battery assembly and long-term fuel cell operation. Besides, PEMs should also possess high toughness because the poor flexibility resulting from rigid aromatic polymer backbones and fluctuation of the environment (*e.g.* working temperature and humidity) often makes them brittle, which can destroy the integrity of PEMs and cause the short circuit of fuel cells. In order to better evaluate the mechanical properties of the obtained PEMs, a tensile test under dry and wet conditions was performed. The representative stress–strain curves and the corresponding data are shown in Fig. 3 and Table 1, respectively. In the dry state, the pure SPEEK membrane exhibited a tensile strength of 68.7 MPa and an elongation at break of about 92%, while the two values for commercial Nafion 115 membranes were 30.4 MPa and 294.4%, verifying that SPEEK is a typical rigid material. However, unlike the decrease in tensile strength in typical PA-doped PEMs, the strength values of SPEEK- $A_x$ /PA and SPEEK- $C_x$ /PA membranes did not show a downward trend but increased slightly. The two series of membranes both demonstrated a strength higher than 70 MPa. The slightly increased strength of these two zwitterionic polymers is related to the ionic crosslinking between the acidic groups ( $-SO_3H$ ) and basic sites (adenine or cytosine) as well as the negligible free PA molecules due to the low doping level of PA. What's more, the two series of membranes exhibited dramatically enhanced flexibility. For example, the highest elongation values of these SPEEK- $A_x$ /PA and SPEEK- $C_x$ /PA membranes can reach 207.5% and 210.1%, respectively. The fracture energy, which can be calculated from the integral area of the stress–strain curve and is usually used to characterize the toughness of materials, and can also prove the enhanced flexibility. The introduction of PA molecules which are mainly

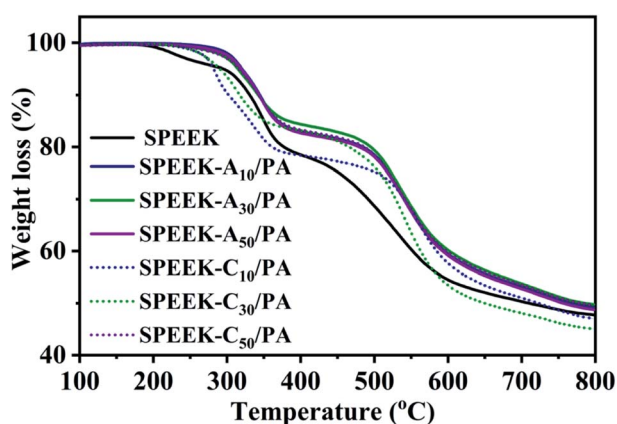


Fig. 2 TGA curves of SPEEK, SPEEK- $A_x$ /PA and SPEEK- $C_x$ /PA membranes.

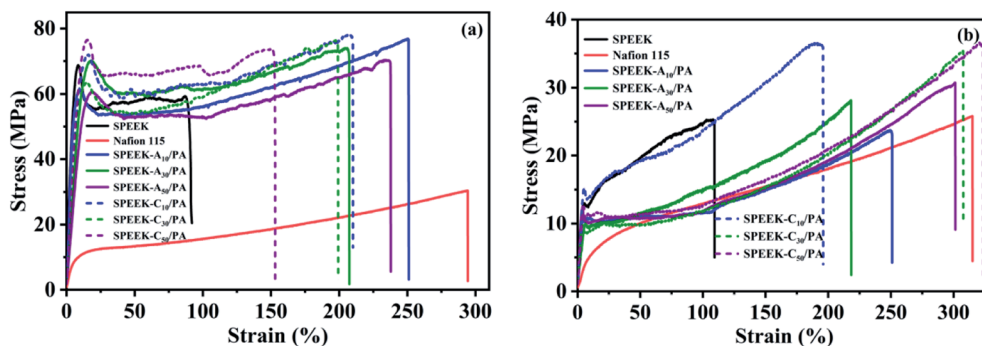


Fig. 3 Typical tensile stress–strain curves of SPEEK, commercial Nafion 115, and the as-prepared PA-doped membranes in (a) the dry state and (b) the wet state.

anchored on the basic sites of the polymer chains weakens the ionic crosslinking between  $\text{SO}_3\text{H}$  groups and the basic sites, thus contributing to a significantly improved toughness.

Considering that the obtained membranes can be used as PEMs in low-temperature PEMFCs, the mechanical properties of these membranes in their hydrate state after soaking in water for 24 h were also evaluated. As expected, all membranes including SPEEK showed decreased strength and increased elongation because the absorbed water molecules play a plasticizer role. However, it is important to note that the SPEEK- $\text{A}_x/\text{PA}$  and SPEEK- $\text{C}_x/\text{PA}$  membranes still possessed satisfactory strength ( $>23.5$  MPa) even if their elongation at break remained at a very high level ( $>200\%$ ). The high strength as well as excellent toughness of the SPEEK- $\text{A}_x/\text{PA}$  and SPEEK- $\text{C}_x/\text{PA}$

membranes in dry and wet states guaranteed their mechanical reliability during battery operation.

### 3.5 Water uptake, swelling and ion exchange capacity (IEC)

The transport of protons in low-temperature PEMFCs strongly depends on the  $\text{H}_2\text{O}$  molecules around ion exchange groups. According to the dominant Grothuss mechanism, protons diffuse along the hydrogen bond network of water molecules or other hydrogen-bonded liquids through the formation/cleavage of these hydrogen bonds.<sup>45</sup> In addition, the vehicle mechanism proposes that  $\text{H}^+$  ions combine with surrounded water molecules to form water-solvated ions ( $\text{H}^+(\text{H}_2\text{O})_x$ ) and then transport by the aid of electro-osmotic drag and concentration gradient.<sup>46</sup> However, high water absorption often brings about excessive

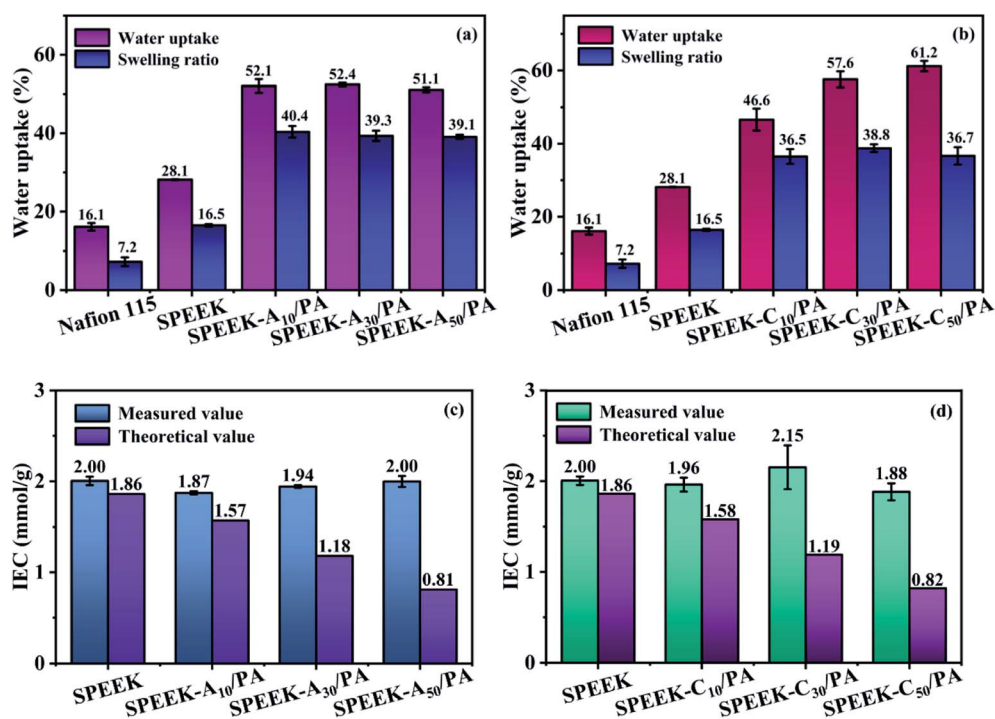


Fig. 4 Water uptake and swelling ratio of (a) SPEEK- $\text{A}_x/\text{PA}$ , and (b) SPEEK- $\text{C}_x/\text{PA}$  membranes. Measured and theoretical IEC values of (c) SPEEK- $\text{A}_x/\text{PA}$  and (d) SPEEK- $\text{C}_x/\text{PA}$  membranes.

swelling and thus results in mechanical damage during the operation. Therefore, moderate water absorption is needed and the water uptake and swelling ratio of the as-prepared SPEEK and PA-doped membranes are shown in Fig. 4a and b. Compared to SPEEK (water uptake of 28.1% and swelling ratio of 16.5%) and commercial Nafion 115 (water uptake of 16.1% and swelling ratio of 7.2%) membranes, the SPEEK-A<sub>x</sub>/PA and SPEEK-C<sub>x</sub>/PA membranes exhibited obviously increased water absorption and a relatively high swelling ratio. Such an increase is due to the hygroscopicity of the doped PA, which possesses high water binding energy. Moreover, the increased hydrogen bond networks formed among different “acid–base” pairs, such as –SO<sub>3</sub>H and –NH–, and PA and –NH–, also contribute to enhance the water absorption capacity to a certain extent. In addition, by comparing the H<sub>2</sub>O absorption and swelling behavior of these two series of membranes with the same grafting ratio, the SPEEK-C<sub>x</sub>/PA membranes demonstrated slightly higher water uptake but a lower swelling ratio, and it is probable that the smaller cytosine molecule is more conducive to the formation of ionic crosslinking. Although the SPEEK-A<sub>x</sub>/PA and SPEEK-C<sub>x</sub>/PA membranes demonstrated higher swelling behavior than SPEEK, it is still acceptable because their swelling ratio values are far below the values (usually beyond 70%) reported in many PA-doped PEMs.<sup>47,48</sup>

IEC refers to the molar content of ions that can be exchanged in ion conductive membranes per unit mass and is generally used to evaluate the ability of membranes to exchange ions. The measured IEC values through acid–base back titration and theoretical IEC values calculated from the SO<sub>3</sub>H content per gram of polymer are presented in Fig. 4c and d. Since the basic sites are not used to calculate the theoretical values, in fact, a large number of PA molecules are immobilized in membranes through acid–base interaction, and the measured IEC values are higher than the theoretical IEC values for all modified SPEEK membranes. With the increase of the degree of substitution of nucleobase, the number of SO<sub>3</sub>H groups gradually decreases, and the theoretical IEC values decrease, but the measured IEC values for all these membranes are similar (~2.0 mmol g<sup>-1</sup>). Therefore, the difference between the measured and the theoretical values increases with the increase of the degree of substitution.

### 3.6 Proton conductivity, PA retention stability, and methanol permeability

The foremost role of PEMs is to conduct working ions (H<sup>+</sup>) from the anode to the cathode. The temperature-dependent proton conductivities are shown in Fig. 5a. All membranes including SPEEK and Nafion 115 showed a monotonic upward trend as a function of temperature, mainly ascribed to the thermally activated H<sup>+</sup> transport process. By comparing the conductivities at the same temperature (e.g. 80 °C), the SPEEK-A<sub>x</sub>/PA and SPEEK-C<sub>x</sub>/PA membranes exhibited ultra-high conductivities (all beyond 220 mS cm<sup>-1</sup>), while the conductivity of SPEEK was only 43.8 mS cm<sup>-1</sup>. The highest conductivity obtained for the SPEEK-C<sub>30</sub>/PA membrane was 276.0 mS cm<sup>-1</sup> at 80 °C, which was 5.3 times higher than that of SPEEK and even 31% higher than that of Nafion 115 (210.7 mS cm<sup>-1</sup>) under the same conditions. Such a significant increase in the proton conductivity of the PA-doped membranes might be not only affected by the increased number of acidic groups due to their similar IEC values to that of SPEEK. In order to find out the reasons for the excellent proton transport ability, we also tested the conductivity of the SPEEK-C<sub>30</sub> membrane without PA doping. In contrast to the super high conductivities of the PA-doped membranes, the un-doped membrane showed a conductivity value as low as 10 mS cm<sup>-1</sup> (80 °C). Based on this result, the absorbed PA molecules plays a vital role in the improvement of proton conductivity. Therefore, due to a higher water uptake and hydration coefficient λ (as shown in Table 1) in the hydrate state, the acidic sites (–SO<sub>3</sub>H and H<sub>2</sub>PO<sub>4</sub><sup>-</sup>) and basic sites (adenine or cytosine) can be easily linked by intermediate H<sub>2</sub>O bridges to form loose acid–base pairs.<sup>49</sup> Thus protons continuously transfer through the alternative formation and breaking of the hydrogen-bonding network among these acid–base pairs *via* the Grotthuss (or hopping) mechanism.<sup>50,51</sup> Additionally, some protons are solvated by free water molecules and then dragged by “vehicles” (H<sub>3</sub>O<sup>+</sup>) *via* the vehicle mechanism.

Although our PA-doped membranes showed excellent proton conductivity under hydration conditions, a key issue, which is the leaching of PA with water in low-temperature PEMFCs during long-term work, is also needed to be considered. To determine the PA retention ability, all SPEEK-A<sub>x</sub>/PA and SPEEK-C<sub>x</sub>/PA membranes were soaked in water at room temperature for 30 days and then tested their conductivities at 80 °C and the

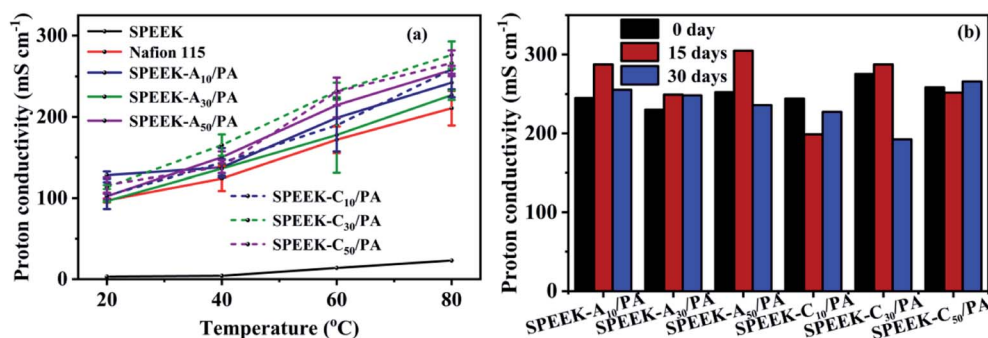


Fig. 5 (a) Proton conductivity vs. temperature at 100% R.H., and (b) proton conductivity (tested at 80 °C) after soaking in water at room temperature up to 30 days.



obtained results are shown in Fig. 5b. Unlike the severe PA loss in most PA-doped PEMs, the SPEEK-A<sub>x</sub>/PA and SPEEK-C<sub>x</sub>/PA membranes showed negligible conductivity change even after soaking for 30 days, verifying the good PA stability in the membranes. This result indicated that there are few free PA molecules in these membranes, and most PA molecules are immobilized around the polymer chains through ionic interaction and hydrogen bonding when at a low PA doping level (Table 1).

In addition to proton conductivity, methanol crossover of a PEM is another key parameter to affect the performance of a DMFC due to many negative effects (*e.g.* fuel waste, mixed potential to reduce the open circuit voltage, catalyst poisoning, *etc.*) caused by methanol permeability. From the result of methanol permeability (Fig. S2<sup>†</sup>), Nafion showed a severe methanol permeability value of about  $14.5 \times 10^{-7} \text{ cm}^2 \text{ s}^{-1}$ , which was also confirmed in our previous work.<sup>17</sup> The large hydrophilic ion clusters of Nafion series membranes, which are originated from their highly phase separated morphology, enable many small polar ions or molecules (*e.g.* H<sup>+</sup> and CH<sub>3</sub>OH) to easily transport through Nafion, thus leading to high conductivity but serious permeability.<sup>52,53</sup> In comparison with

the permeability of SPEEK ( $7.4 \times 10^{-7} \text{ cm}^2 \text{ s}^{-1}$ ), the nucleobase modified SPEEK membranes possess lower methanol permeability and the permeability value of the SPEEK-C<sub>50</sub>/PA membrane decreases to  $1.75 \times 10^{-7} \text{ cm}^2 \text{ s}^{-1}$ . The obviously improved methanol barrier ability of our PA-doped membranes is mainly ascribed to the ionic crosslinking as discussed in the section of mechanical properties.

The ratio of the proton conductivity to the methanol permeability, defined as relative selectivity, is a useful predictive performance parameter to evaluate the potential application in DMFCs.<sup>54</sup> Compared to commercial Nafion 115 and SPEEK, the nucleobase modified SPEEK membranes have exhibited enhanced selectivity. The relative selectivity of the SPEEK-C<sub>50</sub>/PA membrane is up to  $66.4 \times 10^4 \text{ S s cm}^{-3}$ , which is about 9.0 times and 21.9 times higher than that of SPEEK and commercial Nafion 115 membranes, respectively.<sup>17</sup> The high relative selectivity means a low methanol crossover.

### 3.7 DMFC performance

To further prove the practical feasibility of the as-prepared membranes, pure SPEEK, commercial Nafion 115, SPEEK-A<sub>x</sub>/PA and SPEEK-C<sub>x</sub>/PA membranes were each assembled in

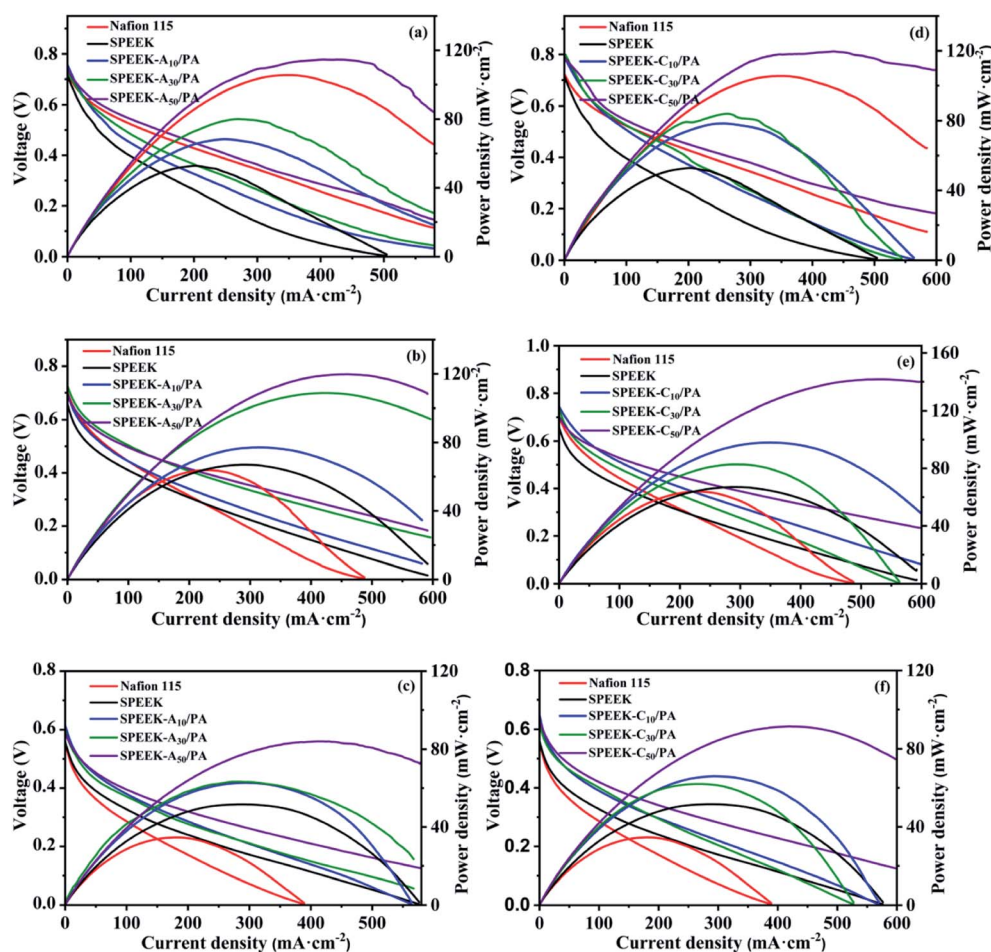


Fig. 6 Polarization and power density curves of SPEEK, SPEEK-A<sub>x</sub>/PA (a–c), SPEEK-C<sub>x</sub>/PA (d–f) and commercial Nafion 115 membranes with 1 M (a and d), 2 M (b and e), and 5 M (c and f) methanol as the fuel at 80 °C (methanol fuel with a flow rate of 1 mL min<sup>-1</sup> and oxygen with a flow rate of 30 mL min<sup>-1</sup>).



Table 2 DMFC performance for different PEMs reported in the literature

| Samples             | $T$ ( $^{\circ}\text{C}$ ) | $C_{\text{MeOH}}$ (M) | OCV (V) | $P_{\text{max}}$ ( $\text{mW cm}^{-2}$ ) | Ref.      |
|---------------------|----------------------------|-----------------------|---------|--|-----------|
| Nafion 117          | 60                         | 2                     | 0.70    | 51.2                                     | 54        |
| CBA/Nafion-PVA4h    | 80                         | 2                     | 0.81    | 68.7                                     | 10        |
| Nafion/FDPA-10      | 60                         | 2                     | 0.72    | 47.3                                     | 44        |
| p-BPAF@Nafion-7.5   | 80                         | 2                     | 0.836   | 111.53                                   | 52        |
| Nafion/SNPAEK-7.5   | 80                         | 2                     | 0.77    | 47                                       | 53        |
| SDF-PAEK@Nafion-15% | 80                         | 2                     | 0.730   | 139                                      | 3         |
| SPEEK/PDA@PVDF      | 70                         | 5                     | 0.64    | 104.0                                    | 17        |
| SPEEK-PSSA-CNT      | 60                         | 2                     | 0.799   | 93                                       | 55        |
| SPEEK-Sfu           | 60                         | 2                     | 0.81    | 103                                      | 56        |
| C-PEEK-25           | 25                         | 4                     | 0.8     | 35.3                                     | 21        |
| SPEEK- $C_{50}$ /PA | 80                         | 2                     | 0.70    | 141.7                                    | This work |

a DMFC single cell as the electrolyte to evaluate the cell performance. Fig. 6 shows the potential–current density and power density–current density curves obtained at 80  $^{\circ}\text{C}$  with 1 M, 2 M, and 5 M methanol as the anode fuel respectively. Generally, a high concentration of the anode fuel means a fast electrode kinetic reaction, but it also leads to the problem of methanol permeability, which brings about many negative effects on the cell performance and fuel utilization. It can be seen that both the SPEEK- $A_x$ /PA and SPEEK- $C_x$ /PA membranes showed higher open-circuit voltages (OCVs) when compared to those of SPEEK especially at higher methanol concentration. For example, the OCVs of SPEEK- $A_{50}$ /PA were 0.75 V (1 M MeOH), 0.70 V (2 M MeOH) and 0.60 V (5 M MeOH), while these values were 0.72 V, 0.66 V and only 0.48 V for SPEEK. This result indicated that the introduction of basic sites into the structure of SPEEK can inhibit the methanol crossover because fuel permeability is the main factor to decrease the OCVs of DMFCs under the same conditions (*e.g.* catalyst loading, the flow rates of the anode fuel and cathode  $\text{O}_2$ , *etc.*).<sup>55,56</sup> As for the maximum power density ( $P_{\text{max}}$ ), the DMFC containing the SPEEK- $C_{50}$ /PA electrolyte output the highest  $P_{\text{max}}$  of 141.7  $\text{mW cm}^{-2}$  among all the samples when feeding 2 M methanol at the anode, whereas Nafion 115 and SPEEK demonstrated a  $P_{\text{max}}$  of only 64.1 and 67.2  $\text{mW cm}^{-2}$ , respectively. Such a more than doubled increase in the power density benefits from the ultra-high proton conductivity together with the good methanol barrier ability of the SPEEK- $A_x$ /PA and SPEEK- $C_x$ /PA membranes. In addition, the DMFC performance of this work is compared with those of recently reported PEMs and the results are summarized in Table 2. The reported SPEEK- $C_{50}$ /PA membrane exhibits significantly higher performance compared with other previously reported PEMs such as commercial Nafion, modified Nafion and other SPEEK membranes, indicating their great potential as PEMs in high-performance DMFCs.

In order to further assess the long-term stability of nucleobase modified SPEEK membranes in DMFCs, the durability of the optimized membrane SPEEK- $C_{50}$ /PA was tested with 2 M MeOH at 80  $^{\circ}\text{C}$  by chronopotentiometry. As shown in Fig. 7, the DMFC with the SPEEK- $C_{50}$ /PA membrane could provide a relatively stable OCV, and it had 89.7% of the initial voltage after 100 h operation at 80  $^{\circ}\text{C}$ . The good stability was mainly due to the acid–base pair interaction between PA molecules and the

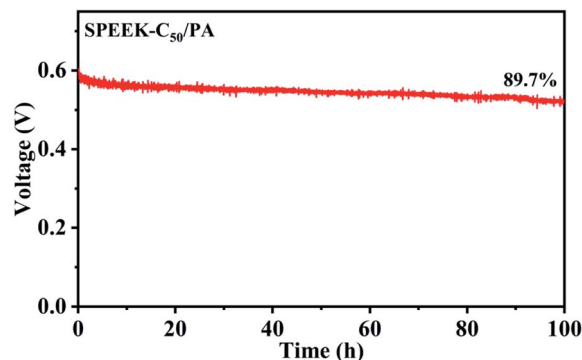


Fig. 7 long-term durability test of the DMFC with the SPEEK- $C_{50}$ /PA membrane under a current density of 300  $\text{mA cm}^{-2}$  with 2 M MeOH at 80  $^{\circ}\text{C}$ .

basic sites on the SPEEK- $C_{50}$  matrix. As reported, commercial Nafion115 as the PEM in DMFCs was tested at 80  $^{\circ}\text{C}$  under a current density of 400  $\text{mA cm}^{-2}$  and showed a 29% loss of voltage after 2.8 h.<sup>57</sup> This indicates that the SPEEK- $C_{50}$ /PA membrane has better stability than Nafion 115 and possesses excellent durability for DMFC applications.

## 4. Conclusions

In summary, two kinds of nucleobase modified SPEEKs with different degrees of substitution, SPEEK- $A_x$  and SPEEK- $C_x$ , were successfully synthesized. Then PA molecules are immobilized through acid–base interaction to fabrication PA-doped polymer membranes. All these PA-doped membranes exhibit sufficient thermal stability and mechanical strength for DMFC applications. In particular, due to the formation of ionic crosslinking caused by the basic sites of nucleobases, the SPEEK- $A_x$ /PA and SPEEK- $C_x$ /PA membranes possess satisfactory strength (>23.5 MPa) even if their elongation at break remained at a very high level (>200%) in the hydrated state. These PA-doped membranes exhibited ultra-high proton conductivities (all beyond 220  $\text{mS cm}^{-1}$ ) at 80  $^{\circ}\text{C}$ , while the conductivity of SPEEK was only 43.8  $\text{mS cm}^{-1}$  with similar IEC values. The acid–base pairs between the acidic sites ( $-\text{SO}_3\text{H}$  and  $\text{H}_2\text{PO}_4^-$ ) and basic

sites (adenine or cytosine) could serve as efficient transportation paths for proton migration and enhance the methanol resistance. The DMFC containing the SPEEK-C<sub>50</sub>/PA electrolyte output the highest  $P_{\max}$  of 141.7 mW cm<sup>-2</sup> when feeding 2 M methanol, more than twice as much as that of the SPEEK membrane (67.2 mW cm<sup>-2</sup>) and Nafion 115 membrane (64.1 mW cm<sup>-2</sup>). Therefore, these results demonstrate that the nucleobase modified membranes have great potential as PEMs for high-performance DMFCs.

## Author contributions

Juan Wu: conceptualization, investigation, visualization, and writing—original draft. Shijun Nie: software, formal analysis, conceptualization, and investigation. Hai Liu: software, resources, and methodology. Chunli Gong: supervision, resources, formal analysis, and writing—review & editing. Quanyuan Zhang: methodology, supervision, project administration, resources, and writing—review & editing. Zushun Xu: methodology. Guangfu Liao: methodology, and writing—review & editing.

## Conflicts of interest

There are no conflicts to declare.

## Acknowledgements

The authors would like to acknowledge the financial support from the National Natural Science Foundation of China (51903078), Key Program of Hubei Provincial Department of Education (D20212703) and Startup Funding for Scientific Research of China University of Geosciences (Wuhan).

## References

- L. Liu, X. Chu, J. Liao, Y. Huang, Y. Li, Z. Ge, M. A. Hickner and N. Li, *Energy Environ. Sci.*, 2018, **11**, 435–446.
- G. Wang, L. Zou, Q. Huang, Z. Zou and H. Yang, *J. Mater. Chem. A*, 2019, **7**, 9447–9477.
- J. Li, F. Bu, C. Ru, H. Jiang, Y. Duan, Y. Sun, X. Pu, L. Shang, X. Li and C. Zhao, *J. Mater. Chem. A*, 2020, **8**, 196–206.
- Y.-J. Wang, W. Long, L. Wang, R. Yuan, A. Ignaszak, B. Fang and D. P. Wilkinson, *Energy Environ. Sci.*, 2018, **11**, 258–275.
- G. Liao, J. Fang, Q. Li, S. Li, Z. Xu and B. Fang, *Nanoscale*, 2019, **11**, 7062–7096.
- M. Hickner, H. Ghassemi, Y. Kim, B. Einsla and J. McGrath, *Chem. Rev.*, 2004, **104**, 4587–4612.
- M. A. Hubert, L. A. King and T. F. Jaramillo, *ACS Energy Lett.*, 2022, **7**, 17–23.
- C. Li and J.-B. Baek, *Nano Energy*, 2021, **87**, 106162.
- H. Zhang and P. Shen, *Chem. Rev.*, 2012, **112**, 2780–2832.
- Y. Li, L. Liang, C. Liu, Y. Li, W. Xing and J. Sun, *Adv. Mater.*, 2018, **30**, 1707146.
- Z. Li and Y.-C. Lu, *Nat. Energy*, 2021, **6**, 517–528.
- W. N. E.-W. Azman, J. Jaafar, W. N. W. Salleh, A. F. Ismail, M. H. D. Othman, M. A. Rahman and F. R. M. Rasdi, *Mater. Today Energy*, 2020, **17**, 100427.
- D. Liu, B. Dong, H. Zhang, Y. Xie, J. Pang and Z. Jiang, *J. Power Sources*, 2021, **482**, 228982.
- P. Das, B. Mandal and S. Gumma, *Chem. Eng. J.*, 2021, **423**, 130235.
- G. Gnanakumar and A. Manthiram, *J. Mater. Chem. A*, 2017, **5**, 20497–20504.
- M. Nguyen, S. Yang and D. Kim, *J. Power Sources*, 2016, **328**, 355–363.
- G. Liu, W. Tseng, S. Jang, F. Hu, F. Zhong, H. Liu, G. Wang, S. Wen, G. Zheng and C. Gong, *J. Membr. Sci.*, 2019, **591**, 117321.
- Z. Xia, X. Zhang, H. Sun, S. Wang and G. Sun, *Nano Energy*, 2019, **65**, 104048.
- C. Zhang, X. Yue, J. Luan, N. Lu, Y. Mu, S. Zhang and G. Wang, *ACS Appl. Energy Mater.*, 2020, **3**, 7180–7190.
- V. Hande, S. Rath, S. Rao, S. Praveen, S. Sasane and M. Patrim, *J. Membr. Sci.*, 2016, **499**, 1–11.
- L. Lei, X. Zhu, J. Xu, H. Qian, Z. Zou and H. Yang, *J. Power Sources*, 2017, **350**, 41–48.
- C. Ru, Z. Li, C. Zhao, Y. Duan, Z. Zhuang, F. Bu and H. Na, *ACS Appl. Mater. Interfaces*, 2018, **10**, 7963–7973.
- J. Han, K. Kim, S. Kim, H. Lee, J. Kim, T. Ko, J. Bae, W. Choi, Y. Sung and J. Lee, *J. Power Sources*, 2020, **448**, 227427.
- X. Liu, S. Zhai, X. Zhang, P. Mao, S. He, W. Dai and J. Lin, *J. Mater. Chem. A*, 2021, **9**, 24044–24055.
- Y. Sui, Y. Du, H. Hu, J. Qian and X. Zhang, *J. Mater. Chem. A*, 2019, **7**, 19820–19830.
- H. Tang, K. Geng, L. Wu, J. Liu, Z. Chen, W. You, F. Yan, M. Guiver and N. Li, *Nat. Energy*, 2022, **7**, 153–162.
- C. Li, Z. Yang, X. Liu, Y. Zhang, J. Dong, Q. Zhang and H. Cheng, *Int. J. Hydrogen Energy*, 2017, **42**, 28567–28577.
- L. Wang, N. Deng, G. Wang, J. Ju, B. Cheng and W. Kang, *ACS Appl. Mater. Interfaces*, 2019, **11**, 39979–39990.
- J. Jiang, X. Zhu, H. Qian, J. Xu, Z. Yue, Z. Zou and H. Yang, *Sustainable Energy Fuels*, 2019, **3**, 2426–2434.
- G. Zhao, X. Xu, L. Shi, B. Cheng, X. Zhuang and Y. Yin, *J. Power Sources*, 2020, **452**, 227839.
- H. Huang, L. Nia, S. Xu, F. Luo, J. Fan, H. Li and H. Wang, *ACS Sustainable Chem. Eng.*, 2021, **9**, 3963–3974.
- M. Song, X. Lu, Z. Li, G. Liu, X. Yin and Y. Wang, *Int. J. Hydrogen Energy*, 2016, **41**, 12069–12081.
- J. Song, Y. Xiao, L. Zhang, J. Xiang, N. Tang, P. Cheng, J. Zhang, S. Wang and W. Du, *Int. J. Hydrogen Energy*, 2021, **46**, 28246–28257.
- H. Li, G. Zhang, W. Ma, C. Zhao, Y. Zhang, M. Han, J. Zhu, Z. Liu, J. Wu and H. Na, *Int. J. Hydrogen Energy*, 2010, **35**, 11172–11179.
- Q. Chen, X. Zuo, H. Liang, T. Zhu, Y. Zhong, J. Liu and J. Nan, *ACS Appl. Mater. Interfaces*, 2020, **12**, 637–645.
- H. Wang, N. Sun, L. Zhang, R. Zhou, X. Ning, X. Zhuang, Y. Long and B. Cheng, *Int. J. Hydrogen Energy*, 2020, **45**, 27772–27778.
- A. Aslan and A. Bozkurt, *Langmuir*, 2010, **26**, 13655–13661.

- 38 Y. Ye, Y. Huang, C. Cheng and F. Chang, *Chem. Commun.*, 2010, **46**, 7554–7556.
- 39 X. Qiu, M. Ueda, H. Hu, Y. Sui, X. Zhang and L. Wang, *ACS Appl. Mater. Interfaces*, 2017, **9**, 33049–33058.
- 40 L. Li, J. Zhang and Y. Wang, *J. Membr. Sci.*, 2003, **226**, 159–167.
- 41 S. Molla and V. Compan, *J. Membr. Sci.*, 2015, **492**, 123–136.
- 42 Q. Che, N. Chen, J. Yu and S. Cheng, *Solid State Ionics*, 2016, **289**, 199–206.
- 43 Y. Yin, J. Wang, S. Jiang, X. Yang, X. Zhang, Y. Cao, L. Cao and H. Wu, *RSC Adv.*, 2015, **5**, 75434–75441.
- 44 Z. Yue, Y. Cai and S. Xu, *J. Membr. Sci.*, 2016, **501**, 220–227.
- 45 Y. Liu, J. Wang, H. Zhang, C. Ma, J. Liu, S. Cao and X. Zhang, *J. Power Sources*, 2014, **269**, 898–911.
- 46 T. Peckham and S. Holdcroft, *Adv. Mater.*, 2010, **22**, 4667–4690.
- 47 H. Bai, H. Peng, Y. Xiang, J. Zhang, H. Wang, S. Lu and L. Zhuang, *J. Power Sources*, 2019, **443**, 227219.
- 48 J. Wang, H. Jiang, Y. Xu, J. Yang and R. He, *Appl. Surf. Sci.*, 2018, **452**, 473–480.
- 49 H. Zhang, Q. Hu, X. Zheng, Y. Yin, H. Wu and Z. Jiang, *J. Membr. Sci.*, 2019, **570–571**, 236–244.
- 50 B. Date, J. Han, S. Park, E. Park, D. Shin, C. Ryu and C. Bae, *Macromolecules*, 2018, **51**, 1020–1030.
- 51 B. Xue, S. Zhou, J. Yao, F. Wang, J. Zheng, S. Li and S. Zhang, *J. Membr. Sci.*, 2020, **594**, 117466.
- 52 C. Ru, Y. Gu, Y. Duan, C. Zhao and H. Na, *J. Membr. Sci.*, 2019, **573**, 439–447.
- 53 B. Wang, L. Hong, Y. Li, L. Zhao, C. Zhao and H. Na, *ACS Appl. Mater. Interfaces*, 2017, **9**, 32227–32236.
- 54 H. Wang, Y. Ma, B. Cheng, W. Kang, X. Li, L. Shi, Z. Cai and X. Zhuang, *Electrochim. Acta*, 2017, **258**, 24–33.
- 55 G. Rambabu and S. D. Bhat, *Chem. Eng. J.*, 2014, **243**, 517–525.
- 56 G. Rambabu and S. D. Bhat, *Electrochim. Acta*, 2015, **176**, 657–669.
- 57 H. Huang, Y. Ma, Z. Jiang and Z. Jiang, *J. Membr. Sci.*, 2021, **636**, 119585.